Article published online: 2024-12-30

Mechanism of Action of the Traditional Chinese Medicine Formula Weichang'an in the Treatment of Gastric Cancer Based on TMT Proteomics Analysis

Yaofei Niu[1] Weixia Chen[2,3] Yajie Ding[2] Yan Xu[2] Aiguang Zhao[2]

[1] Department of Infection, Henan Provincial People's Hospital, Zhengzhou, Henan, China
[2] Department of Oncology, Longhua Hospital Affiliated to Shanghai University of Traditional Chinese Medicine, Shanghai, China
[3] Department of Oncology, Henan Province Hospital of TCM (The Second Affiliated Hospital of Henan University of Chinese Medicine), Zhengzhou, Henan, China

Address for correspondence Aiguang Zhao, PhD, Department of Oncology, Longhua Hospital Affiliated to Shanghai University of Traditional Chinese Medicine, 725 Wanping South Road, Xuhui District, Shanghai, China (e-mail: aiguangzhao@qq.com).

CMNP 2024;4:e173–e181.

Abstract

Objective The aim of the study was to screen key proteins involved in the treatment of human gastric cancer subcutaneous xenografts in nude mice by the traditional Chinese medicine formula Weichang'an and to explore its mechanism of action in treating gastric cancer.

Methods Sixteen 7- to 8-week-old female BALB/C nude mice were used to establish a human gastric cancer subcutaneous xenograft model by bilateral axillary injection of MKN45 cells. Mice with successfully established tumors were randomly divided into the Weichang'an group and the model group, with eight mice in each group. Mice in the Weichang'an group were orally administered 0.5 mL of Weichang'an decoction, while mice in the model group were given 0.5 mL of normal saline by gavage once a day for 21 consecutive days. On day 28, the animals were sacrificed by cervical dislocation, and tumors were excised to measure tumor weight and assess the tumor suppression rate. Tandem mass tags (TMT) quantitative proteomics was used to analyze the tumor samples, identify differentially expressed proteins, and perform Gene Ontology (GO) and Kyoto Encyclopedia of Genes and Genomes (KEGG) pathway enrichment analysis.

Results Compared with the model group, the tumor weight in the Weichang'an group was significantly reduced ($p < 0.001$), and the tumor suppression rate was 41.40%, indicating that Weichang'an can inhibit the growth of human gastric cancer subcutaneous xenografts in nude mice. TMT quantitative proteomics identified a total of 2,856 proteins, with 13 proteins showing downregulated expression and 25 proteins showing upregulated expression in the Weichang'an group. GO enrichment analysis revealed that differentially expressed proteins were mainly enriched in cellular components such as the cell membrane, extracellular matrix, and envelope, and participated in biological processes like negative regulation of cell adhesion,

Keywords
- TMT proteomics
- Weichang'an
- gastric cancer
- differentially expressed protein

received
August 11, 2024
accepted after revision
September 22, 2024

DOI https://doi.org/10.1055/s-0044-1801293.
ISSN 2096-918X.

© 2024. The Author(s).
This is an open access article published by Thieme under the terms of the Creative Commons Attribution License, permitting unrestricted use, distribution, and reproduction so long as the original work is properly cited. (https://creativecommons.org/licenses/by/4.0/)

Georg Thieme Verlag KG, Oswald-Hesse-Straße 50, 70469 Stuttgart, Germany

hematopoiesis, and skeletal system development, with functions in cell adhesion molecule binding and molecular sensor activity. The KEGG pathway enrichment analysis identified the autophagy-lysosome pathway.

Conclusion Weichang'an may exert its therapeutic effect on gastric cancer by regulating the expression of various proteins and modulating the autophagy-lysosome pathway.

Introduction

On February 1, 2024, the International Agency for Research on Cancer (IARC) released the latest global cancer statistics. By 2022, there were an estimated 20 million new cancer cases and nearly 10 million cancer-related deaths worldwide. Among these, there were 970,000 new cases of gastric cancer and 660,000 deaths, ranking fifth in both incidence and mortality rates.[1] In China, the detection rate of early-stage gastric cancer remains low, and most patients are diagnosed at an advanced stage, losing the opportunity for curative resection, which results in poor prognosis. Traditional chemotherapy and radiation therapies have limited efficacy. Due to the high spatiotemporal heterogeneity of gastric cancer, progress in precise targeted therapies has been slow.[2] Traditional Chinese medicine (TCM) plays an important role in the prevention and treatment of gastric cancer. Our research team has developed a TCM compound, Weichang'an, which primarily strengthens the spleen, targeting the major pathogenic factor of spleen and stomach deficiency. This formulation has been used clinically for nearly 30 years as an in-hospital preparation and has shown definitive efficacy in improving the spleen deficiency syndrome in gastric cancer patients, extending survival, and reducing recurrence and metastasis after radical surgery.[3–5]

With advancements in medical technology, research in TCM has also deepened, with the ultimate goal of enhancing clinical efficacy, improving patient quality of life, and prolonging survival. High-throughput screening technologies are increasingly used in scientific research, and proteomics has become an indispensable tool in functional genomics. It not only provides potential biomarkers for diagnosis but also offers insights for better understanding the mechanisms of TCM in treating diseases. Tandem mass tags (TMT) technology, developed by Thermo Fisher Scientific in the United States, is a high-throughput proteomics technique that labels peptide amino groups with 2 to 10 stable isotopes for mass spectrometry analysis.[6] This study aims to identify key proteins involved in the treatment of human gastric cancer in nude mice with the TCM compound Weichang'an, using proteomics to explore the biological basis of its effect on gastric cancer and provide a reference for further understanding its therapeutic mechanisms.

Materials

Experimental Animals and Cells

Sixteen 7- to 8-week-old female BALB/C nude mice, weighing 16 to 20 g, were provided by the Animal Facility of the Shanghai Cancer Institute, with animal production license number SCXK (Hu) 2002–0001. The animals were housed and experiments were conducted in strict accordance with specific pathogen-free (SPF) standards. The animal facility had the license number SYXK (Hu) 2002–0009. The animal experiment was approved by the Ethics Committee of Experimental Animals at Shanghai University of Traditional Chinese Medicine, with ethical approval number LHERAW-20003. The human gastric cancer cell line MKN45 was kindly provided by the Department of Pharmacy, East China University of Science and Technology.

Reagents

The reagents used in the study were the following: Triton X-100 (MedChemExpress, USA, CAS number: 9002–93–1); DL-dithiothreitol (DTT), trifluoroacetic acid (TFA), iodoacetamide (IAA), ammonium bicarbonate (NH_4HCO_3), N,N,N',N'-tetramethylethylenediamine (TEMED), urea (Sigma-Aldrich, USA, product numbers: 43819, T6508, V900335, A6141, T8133, U5128); TMT labeling kit, Pierce Dilution-Free Rapid Gold BCA Protein Assay, Thermo Fisher Scientific, USA, catalog number: A58332, A55861); trypsin (Promega, USA, catalog number: V5113); acetonitrile (Merck, Germany, product number: 1.00030); formic acid (FA; Millipore, USA, product number: 5.33002); BCA protein concentration assay kit (Shanghai Beyotime Biotechnology Co., Ltd., China, product number: P0012); tetraethylammonium bromide [TEAB; Qi Yi Biotechnology (Shanghai) Co., Ltd., China, catalog number: 71–91–0].

Instruments

The instruments used were the following: Q Exactive HF-X quadrupole-Orbitrap liquid chromatography-mass spectrometry system, EASY-nLC1200 chromatography system, Multiskan FC microplate reader (Thermo Fisher Scientific, USA); JY96-IIN ultrasonic cell crusher (Ningbo XinZhi Biotechnology Co., Ltd., China); and PowerPac electrophoresis system (BIO-RAD, USA).

Methods

Preparation of Weichang'an

The TCM compound formula Weichang'an consists of 12 g of Taizishen (Pseudostellariae Radix), 12 g of fried Baizhu (Atractylodis Macrocephalae Rhizoma), 15 g of Fuling (Poria), 9 g of Xiakucao (Prunellae Spica), 9 g of Jiang Banxia (Pinelliae Rhizoma Praeparatum cum Zingibere et alumine), 9 g of Chenpi (Citri Reticulatae Pericarpium), 30 g of Hongteng (Sargentodoxae Caulis), 30 g of wild Putaoteng (Vitis

quinquangularis Rehd), 3 Bihu (*Gekko japonicus* Dumeril et Bibron), 30 g of Sheng Muli (Ostreae Concha), and 9 g of Lyu Emei (*Prunus mume* Sieb. et Zucc). The TCM decoction pieces were provided and identified by the TCM Pharmacy at Longhua Hospital, Shanghai University of Traditional Chinese Medicine. Weichang'an water extract was prepared using the decoction method, with the drug concentration adjusted to 240 g/L (per liter of crude drug), sterilized at high temperature, and stored at 4°C for later use. High-performance liquid chromatography (HPLC) was used to quantitatively measure the active ingredient hesperidin in the Weichang'an decoction to assess its quality.[7]

Establishment of Subcutaneous Tumor Model in Nude Mice and Grouping

The MKN45 cell line was expanded in culture, and 1×10^7 cells were suspended in 0.2mL serum-free culture medium. The cell suspension was injected subcutaneously into the axillae of nude mice (0.1 mL per side). On the seventh day postinjection, noticeable tumor nodules appeared at the injection sites, indicating successful establishment of the tumor model. Mice with successful tumor formation were randomly divided into two groups: the Weichang'an group and the model group, with eight mice each group. Mice in the Weichang'an group were orally administered 0.5 mL of Weichang'an decoction, while those in the model group were given 0.5 mL of normal saline, once daily for 21 days. On the 28th day of the experiment, the mice were euthanized by cervical dislocation, the tumors were excised, and then immediately frozen.

Protein Sample Preparation

Mouse tumor samples were taken from the –80°C freezer and ground into powder using liquid nitrogen. Each group of samples was mixed with four times the volume of lysis buffer (containing 8 mol/L urea and 1% protease inhibitor) and subjected to ultrasonic lysis. The samples were then centrifuged at 12,000 × *g* for 10 min at 4°C, and the supernatant was collected. Protein concentration was determined using a bicinchoninic acid (BCA) protein assay kit. A protein solution of 80 µg was mixed with DTT to achieve a final concentration of 5 mmol/L and reduced at 56°C for 30 min. IAA was then added to a final concentration of 11 mmol/L, and the mixture was incubated at room temperature for 15 min in the dark. Finally, the samples were diluted to a concentration lower than 2 mol/L. Trypsin was added at a mass ratio of 1:50 (trypsin:protein) and incubated at 37°C overnight for digestion. Afterward, 1% trypsin was added for a further 4 h of digestion. The trypsin-digested peptides were desalinated using a Strata X C18 column (Phenomenex), and the desalinated peptides were vacuum freeze-dried. The peptides were then dissolved in 0.5 mol/L TEAB and labeled using the TMT reagent kit according to the manufacturer's instructions.

HPLC Fractionation

Peptides were fractionated using high pH reverse-phase liquid chromatography with an Agilent 300Extend C18 column (particle size of 5 µm, inner diameter of 4.6 mm, length of 250 mm). The labeled peptides from each group were mixed and fractionated using an Agilent 1260 infinity II HPLC system. The mobile phase A consisted of 10 mmol/L $HCOONH_4$, 5% CAN, pH 10.0, and phase B was 10 mmol/L $HCOONH_4$, 85% CAN, pH 10.0. The column was equilibrated with mobile phase A, and the sample was injected using an autosampler for separation on the column at a flow rate of 1 mL/min. The gradient elution conditions were as follows: 0 to 25th minutes, 0% B; 25th to 30th min, linear gradient 0 to 7% B; 30th to 65th min, linear gradient 7% to 40% B; and 65th to 70th min, linear gradient 40% to 100% B; 70th to 85th min, 100% B. The elution was monitored at 214 nm, and fractions were collected every minute, yielding approximately 40 fractions. After freeze-drying, the samples were redissolved in 0.1% FA and combined into different fractions.

Liquid Chromatography-Mass Spectrometry Analysis

The combined peptide fractions were dissolved in mobile phase A (0.1% FA aqueous solution) and separated using an EASY-nLC 1200 ultra-HPLC system. The mobile phase B was 0.1% FA acetonitrile solution. The liquid chromatography gradient was as follows: 0 to 60th min, 6% to 20% B; 60th to 80th min, 20% to 30% B; 80th to 86th min, 30% to 80% B; and 86th to 90th min, 80% B, with a flow rate maintained at 350 nL/min. After separation by ultra-HPLC, peptides were ionized using an NSI ion source and analyzed using an Orbitrap Fusion Lumos mass spectrometer. The ion source voltage was set to 2.4 kV, and both the parent ions and their fragment ions were analyzed by high-resolution Orbitrap. Data were collected using data-dependent acquisition (DDA) mode, with automatic gain control (AGC) set to 5×10^4, a signal threshold of 5,000 ions/s, and a maximum injection time of 100 ms. The dynamic exclusion time for tandem mass spectrometry scans was set to 30 s to prevent repetitive scanning of parent ions.

Data Processing

Secondary mass spectrometry data were searched using the MaxQuant database. The search parameters were set to SwissProt Human (20,130 sequences) and SwissProt Mouse (16,839 sequences), with a reverse database included to calculate the false-positive rate due to random matches. Common contaminant databases were also added. The enzyme digestion method was set to trypsin/P; the maximum number of missed cleavages was set to 2; the minimum peptide length was set to 7 amino acid residues; the maximum number of modifications per peptide was set to 5. The mass tolerance for the primary parent ion was set to 5 ppm for Main search and 20 ppm for First search, and the mass tolerance for secondary fragment ions was set to 0.02 Da. Cysteine alkylation was set as a fixed modification, while variable modifications included methionine oxidation and N-terminal acetylation of the protein. The quantification method used was TMT-10plex, and the false-positive rates for PSM identification and protein identification were both set to 1%. Differential proteins were screened using the *p*-value and fold change parameters. Gene Ontology (GO) and

Table 1 Effect of Weichang'an on subcutaneous tumor growth in nude mice ($\bar{x} \pm S$)

Group	*n*	Tumor mass (m/g)	*p*-value	Tumor inhibition rate/%
Model group	8	2.15 ± 0.24	0.000	41.40
Weichang'an group	8	1.26 ± 0.11		

Kyoto Encyclopedia of Genes and Genomes (KEGG) databases were used for enrichment analysis of the differential proteins. GO analysis described the proteins from three dimensions: molecular function, biological process, and cellular component. Fisher's exact test was used to calculate and select significantly different protein pathways.

Statistical Analysis

Data were analyzed using SPSS 22.0 software, and results were expressed as mean ± standard deviation ($\bar{x} \pm s$). The study compared two groups, and since the data met normality tests, independent sample *T*-tests were used. A *p*-value of less than 0.05 was considered statistically significant.

Results

Weichang'an Inhibits Subcutaneous Tumor Growth in Human Gastric Cancer Nude Mice

Compared with the model group, the tumor weight of the nude mice in the Weichang'an group was significantly reduced, with a statistically significant difference ($p = 0.000$), and the tumor inhibition rate was 41.40%. This indicates that Weichang'an can inhibit the growth of subcutaneous transplanted tumors in human gastric cancer nude mice (see ►**Table 1**).

Differential Protein Identification

Proteomic analysis identified differential expression proteins in human gastric cancer nude mice subcutaneous transplanted tumors after intervention with the compound Weichang'an. A total of 2,856 proteins containing quantitative information were identified. Proteins with a fold change greater than 1.2 were considered significantly upregulated, and those with a fold change less than 0.83 were considered significantly downregulated. Among the quantified proteins, 13 proteins were significantly downregulated and 25 proteins were significantly upregulated in the Weichang'an group (see ►**Fig. 1** and ►**Tables 2** and **3**).

Differentially Expressed Protein Enrichment Analysis

GO and KEGG enrichment analyses were performed on the differentially expressed proteins, and the significance of these proteins in specific functional annotations was evaluated. GO enrichment analysis of the differentially expressed proteins was conducted using the GO database. The results showed that, in terms of cellular components, the differentially expressed proteins were primarily enriched in the cell membrane, extracellular matrix, and envelope. In terms of molecular functions, the differentially expressed proteins were primarily enriched in cell adhesion molecule binding, extracellular matrix structural components, signal receptor activity, and molecular sensor activity. In terms of biological processes, the differentially expressed proteins were mainly enriched in the negative regulation of cell adhesion, hematopoiesis, development of the skeletal system, and cellular responses to stimuli such as peptide hormones, epidermal growth factor, and insulin-like growth factor (see ►**Fig. 2**). KEGG enrichment analysis of the differentially expressed proteins was performed using the KEGG database to predict the signaling pathways involved in these proteins, thereby

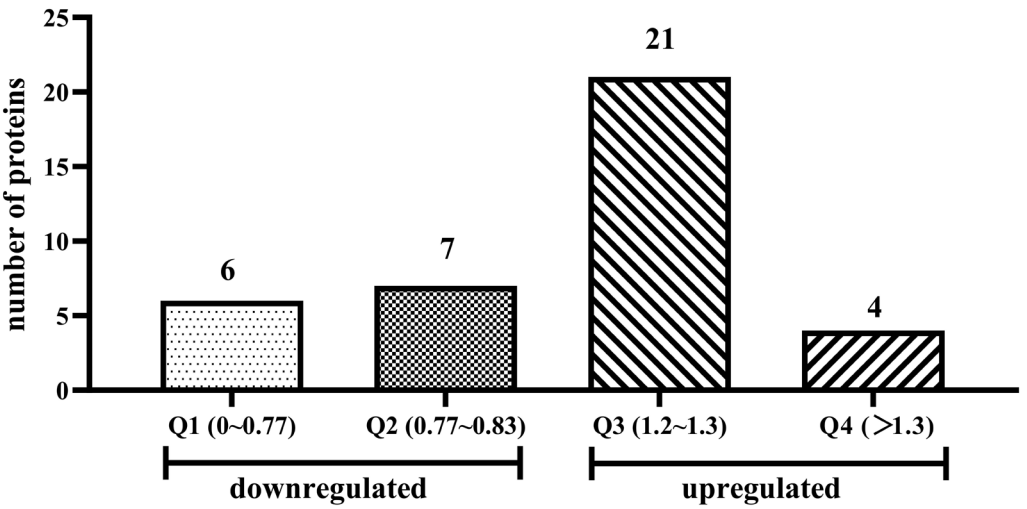

Fig. 1 Number of differentially expressed proteins at different thresholds.
Notes: Q1 (0~0.77): fold change range from 0 to 0.77; Q2 (0.77~0.83): fold change range from 0.77 to 0.83; Q3 (1.2~1.3): fold change range from 1.2 to 1.3; Q4 (>1.3): fold change range greater than 1.3. The numbers on each bar represent the number of proteins in each range.

 © 2024. The Author(s).

Table 2 Differential proteins with downregulated expression in the Weichang'an group

No.	Names of differential proteins	Fold change	*p*-value
1	Glyceraldehyde-3-phosphatedehydrogenase, testis-specific	0.761	0.006
2	Serine/threonine-protein kinase Chk1	0.572	0.010
3	Ribosomal L1 domain-containing protein 1	0.741	0.035
4	Complement factor D	0.813	0.041
5	Collagen α-1(I) chain	0.749	0.038
6	Clathrin light chain A	0.79	0.010
7	Fibrillin-1	0.77	0.003
8	Interferon-induced protein with tetratricopeptide repeats 5	0.809	0.016
9	Ribosome production factor 2 homolog	0.675	0.037
10	G-protein coupled receptor family C group 5 member C	0.781	0.018
11	1-acyl-sn-glycerol-3-phosphate acyltransferase epsilon	0.811	0.009
12	Lysosomal thioesterase PPT2	0.811	0.031
13	Feline leukemia virus subgroup C receptor-related protein 1	0.73	0.019

Table 3 Differential proteins with upregulated expression in the Weichang'an group

No.	Names of differential proteins	Fold change	*p*-value
1	PDZ and LIM domain protein 1	1.241	0.006
2	Tumor protein D54	1.214	0.019
3	Putative nucleoside diphosphate kinase	1.345	0.012
4	Steroid hormone receptor ERR2	2.255	0.029
5	Protein-L-isoaspartate (D-aspartate) O-methyltransferase	1.202	0.047
6	Cofilin-1	1.244	0.001
7	Tyrosine-protein phosphatase nonreceptor type 6	1.269	0.014
8	Lysosomal acid lipase/cholesteryl ester hydrolase	1.275	0.046
9	Basal cell adhesion molecule	1.261	0.029
10	Myomesin-1	1.317	0.014
11	UV excision repair protein RAD23 homolog B	1.201	0.026
12	Tumor protein D52	1.219	0.020
13	Cytochrome c oxidase assembly factor 6 homolog	1.238	0.048
14	Calmodulin-lysine N-methyltransferase	1.245	0.006
15	Plasminogen activator inhibitor 1 RNA-binding protein	1.302	0.027
16	Coiled-coil domain-containing protein 12	1.239	0.046
17	Uncharacterized protein KIAA1143	1.284	0.010
18	Carboxymethylenebutenolidase homolog	1.235	0.032
19	Transcription elongation factor A protein-like 4	1.245	0.038
20	Serine/arginine-related protein 53	1.223	0.001
21	Nonstructural maintenance of chromosomes element 3 homolog	1.247	0.024
22	Equilibrative nucleoside transporter 1	1.226	0.028
23	Zinc finger protein 106	1.217	0.027
24	Ubiquitin-like conjugating enzyme ATG3	1.228	0.002
25	Epidermal growth factor receptor substrate 15-like 1	1.236	0.044

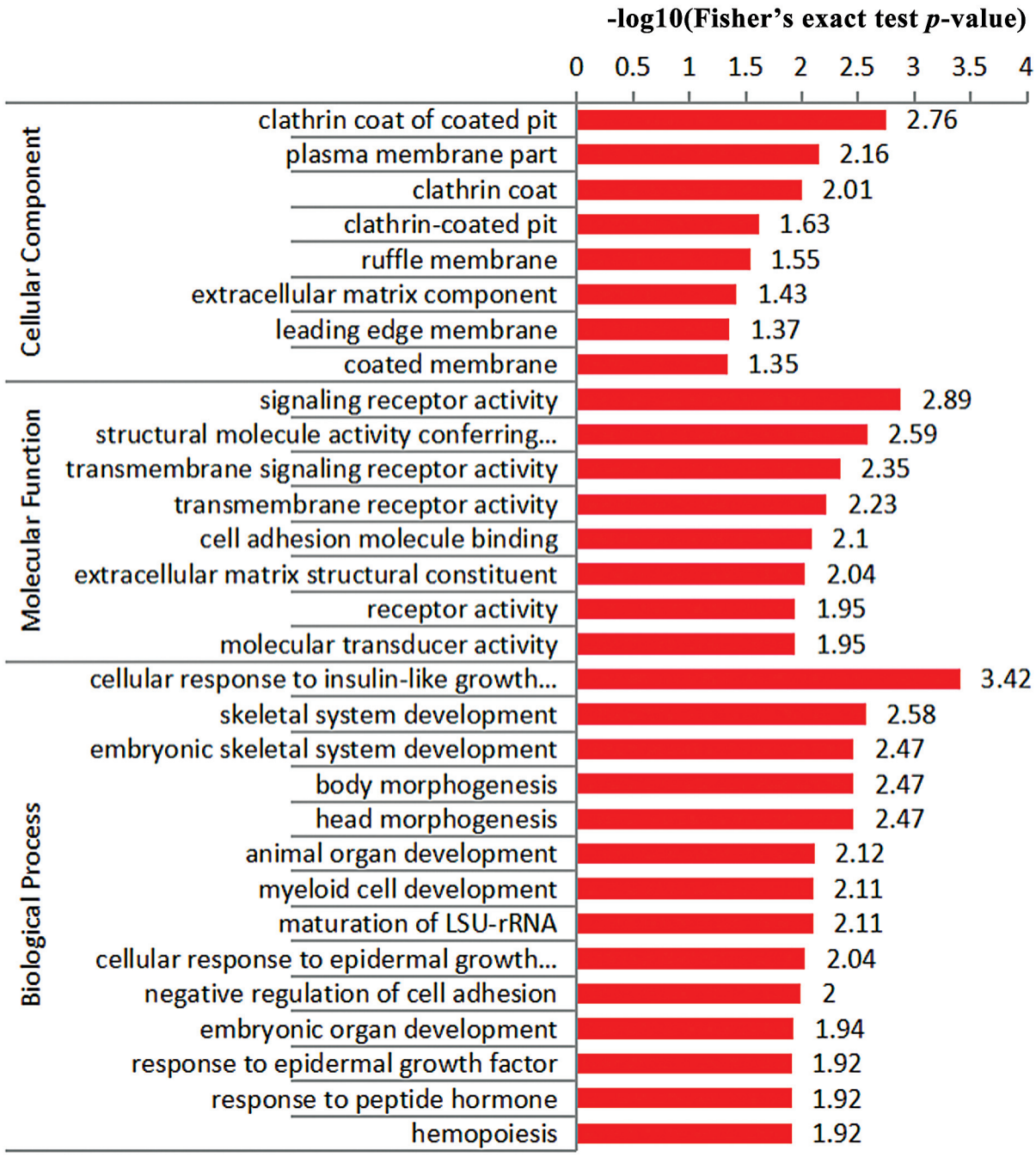

Fig. 2 Gene Ontology enrichment analysis of differential proteins.

revealing the mechanism of action of the Weichang'an formula in the treatment of gastric cancer. Pathway annotation of the differentially expressed protein genes based on the KEGG database identified all the pathways associated with the differentially expressed proteins, and pathways significantly related to the differentially expressed proteins were selected with $p < 0.05$, with lysosome signaling pathway being identified as a significant pathway (see ►**Fig. 3**).

Discussion

TCM treatment for advanced gastric cancer not only acts synergistically with chemotherapy drugs to enhance efficacy and reduce toxicity but also plays a role in prolonging survival and improving quality of life. Through long-term clinical practice and basic research, under the guidance of TCM theory, Prof. Qiu proposed the academic concept that "spleen deficiency is key in gastric cancer" and that

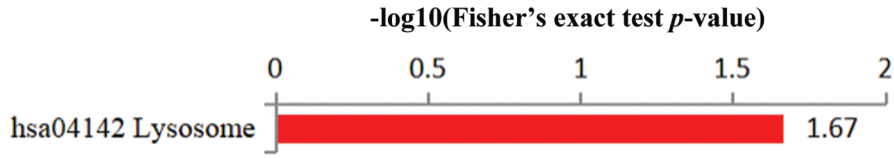

Fig. 3 KEGG signaling pathway enrichment analysis of differential proteins.

"tonifying the spleen is essential throughout the treatment process," which led to the formulation of the TCM compound Weichang'an. In this formula, herbs like Taizishen (Pseudostellariae Radix), Baibiandou (Lablab Semen Album), Baizhu (Atractylodis Macrocephalae Rhizoma), and Fuling (Poria) serve as the main ingredients, primarily exerting effects on tonifying the spleen and regulating qi. Herbs such as Hongteng (Sargentodoxae Caulis) and Baqia (Smilacis Chinae Rhizoma) act as adjuncts for clearing heat and detoxifying; raw Muli (Ostreae Concha) and Xiakucao (Prunellae Spica) help soften masses and resolve phlegm, while Jiangbanxia (Pinelliae Rhizoma Praeparatum cum Zingibere et alumine), Qingpi (Citri Reticulatae Pericarpium Viride), and Chenpi (Citri Reticulatae Pericarpium) work to harmonize the stomach and regulate qi. Although the efficacy of Weichang'an in treating gastric cancer is significant, its underlying mechanism is not yet fully understood. With the continuous advancement of high-throughput screening technologies, proteomics has made important contributions to the modernization of TCM research, particularly in exploring disease-related biomarkers and targets, with quantitative proteomics being widely used for this purpose.[8,9]

TMT is a high-throughput proteomics technology developed by Thermo Fisher Scientific in the United States. It involves mass spectrometry analysis of peptides labeled with 2 to 10 stable isotopes. This method offers several advantages, including short run times, simple operation steps, simultaneous analysis of multiple samples, high protein identification, and good result reproducibility.[10] In this study, TMT labeling, HPLC fractionation, and quantitative proteomics techniques were used to analyze the impact of gastrointestinal agents on protein expression in gastric cancer subcutaneous xenograft tumors, exploring the mechanism of gastrointestinal treatment in gastric cancer at the protein level. A total of 3,385 proteins were identified based on TMT quantitative proteomics, of which 2,856 proteins contained quantitative information. Among the quantified proteins, 13 proteins were downregulated and 25 proteins were upregulated in the gastrointestinal agent–treated group. Further literature analysis of the differential proteins revealed that these proteins were mainly related to the cytoskeleton, cell cycle, DNA damage repair, and autophagy.

PDZ and LIM domain protein 1 (PDLIM1), also known as CLP-36, is a member of the PDZ-LIM family of adaptor proteins. It is associated with the cytoskeleton, neuronal signal transduction, organ development, and tumorigenesis.[11] Studies have shown that PDLIM1 is involved in the invasion, migration, and metastasis of tumor cells in breast cancer, colon cancer, and gliomas.[12–14] Serine/threonine-protein kinase Chk1 (CHEK1), also known as checkpoint kinase 1, is a key protein that controls the cell cycle and DNA stability. It is essential for checkpoint-mediated cell cycle arrest in response to DNA damage or unreplicated DNA, regulating cell cycle checkpoints and coordinating DNA repair.[15,16] Research has found that high expression of CHEK1 is associated with poor prognosis in patients with non-small-cell lung carcinoma (NSCLC) and also has a similar correlation in ovarian cancer.[17,18] Fibrillin-1 (FBN1) is a structural component of microfibrils in the extracellular matrix, serving as an important and complex lattice protein that regulates the microenvironment.[19–21] Recent studies have shown that FBN1 is closely related to tumorigenesis and progression. Silencing FBN1 expression can reduce proliferation and induce apoptosis in thyroid papillary carcinoma cells. High expression of FBN1 may induce early recurrence of ovarian cancer and sensitivity to platinum-based chemotherapy.[22,23] Ribosomal L1 domain-containing protein 1 (RSL1D1), also known as cellular senescence-inhibited gene protein (CSIG), is involved in regulating multiple biological processes such as the cell cycle, cellular senescence, apoptosis, and tumor metastasis. Studies have shown that RSL1D1 is highly expressed in liver cancer and prostate cancer tissues, and its expression is associated with poor prognosis in patients.[24,25] Collagen α-1 (I) chain (COL1A1), also known as α-1 type I collagen, is a major component of the extracellular matrix, primarily maintaining the integrity of the cytoskeletal structure. Its degradation is an important process in the invasion and metastasis of tumor cells.[26,27] COL1A1 is highly expressed in gastric cancer tissues and is positively correlated with tumor cell invasion and metastasis.[28] Silencing COL1A1 in gastric cancer BGC-823 cells can inhibit tumor cell proliferation and migration ability.[29] Cofilin-1 (CFL1), a low-molecular-weight actin-regulating protein,[30] plays an important role in cell proliferation and migration and is a key regulator in tumor cell invasion and metastasis.[31] Recent studies have found that CFL1 is highly expressed in various tumor tissues, including renal cell carcinoma, ovarian cancer, oral squamous cell carcinoma, pancreatic cancer, and breast cancer.[32–34] Clinical studies show that CFL1 is closely associated with pathological differentiation, tumor size, lymph node metastasis, and clinical staging in gastric cancer, and plays an important role in tumor cell invasion and metastasis.[35] Ultraviolet (UV) excision repair protein RAD23 homolog B (RAD23B) is involved in nucleotide excision repair. Increasing evidence suggests that tumorigenesis is associated with the expression levels of DNA repair genes. The expression level of HR23B, the protein encoded by the *RAD23B* gene, is closely related to tumor invasion and prognosis. Genome-wide association studies have demonstrated that single nucleotide polymorphism

(SNP) in *RAD23B* are associated with esophageal cancer and bladder cancer.[36,37] Plasminogen activator inhibitor 1 RNA-binding protein (SERBP1) plays a central role in fibrinolysis, angiogenesis, wound healing, and tumor cell invasion and metastasis.[38,39] Recent studies have found that SERBP1 is significantly overexpressed in ovarian cancer epithelial cells and is strongly correlated with advanced tumor staging.[40] In contrast, overexpression of SERBP1 is positively correlated with a good prognosis in human breast cancer, suggesting that SERBP1 may have a potential protective role in breast cancer progression.[41] Equilibrative nucleoside transporter 1 (SLC29A1), a member of the solute carrier (SLC) transporter family, is a type of membrane transporter.[42] The SLC superfamily plays an important role in the homeostasis of endogenous compounds, drug delivery, and tumor drug resistance.[43,44] The study found that the expression of SLC29A1 is positively correlated with the chemotherapy efficacy in Asian pancreatic cancer patients;[44] significant upregulation of SLC29A1 in colorectal cancer, astrocytoma, and breast cancer cells helps reduce cisplatin resistance and enhances cell viability;[45] silencing the expression of SLC29A1 reduces the drug sensitivity in leukemia and lung cancer cells.[46] The ubiquitin-like conjugating enzyme ATG3, also known as autophagy-related gene 3, plays a key role in the formation of autophagosomes.[47] During the autophagic process, microtubule-associated protein 1 light chain 3-I (LC3-I) is converted into the ubiquitin-like conjugating enzyme ATG3, and with the help of ATG5-ATG12-ATG16, it is lipidated into LC3-II. Studies have shown that silencing ATG3 expression reduces autophagic activity and inhibits the migration ability of NSCLC, possibly by inhibiting the activation of the Notch/snail signaling pathway, thereby affecting the process of epithelial–mesenchymal transition (EMT).[48]

GO enrichment analysis revealed that the differentially expressed proteins were mainly enriched in cellular components such as the cell membrane, extracellular matrix, and envelope. These proteins participate in biological processes such as the negative regulation of cell adhesion, hematopoiesis, skeletal system development, and cellular responses to stimuli such as peptide hormones, epidermal growth factor, and insulin-like growth factor. They play roles in functions such as cell adhesion molecule binding, extracellular matrix structural component, receptor activity, and molecular sensor activity. KEGG enrichment analysis identified the lysosome pathway as a key signaling pathway. Studies have shown that autophagic dysfunction is closely related to tumor occurrence and malignant transformation.[49] Depending on the cellular conditions and the duration and intensity of stress stimuli, autophagy can either suppress or promote cancer cell death. Moreover, inhibiting autophagy can increase the sensitivity of tumor cells to chemotherapy drugs and radiotherapy.[50]

Conclusion

This study, through proteomics, found that cytoskeleton-related proteins, cell cycle–related proteins, and autophagy-related proteins may be involved in the inhibitory effect of Weichang'an on human gastric cancer cells, and elucidates the biological basis of Weichang'an in the treatment of gastric cancer. In the future, we will further conduct experimental studies on the treatment of gastric cancer with Weichang'an, focusing on cytoskeleton proteins that inhibit invasion and metastasis, as well as autophagy-lysosome-related pathways. We aim to explore the molecular mechanisms underlying Weichang'an's treatment of gastric cancer and identify key intervention targets in gastric cancer treatment so as to provide further evidence for the prevention and treatment of gastric cancer.

CRediT Authorship Contribution Statement

Yaofei Niu contributed to project administration, conceptualization, data curation, formal analysis, and writing the original draft. Weixia Chen and Yajie Ding contributed to funding acquisition, investigation, data curation, formal analysis, validation, and methodology. Yan Xu and Aiguang Zhao contributed to project administration, supervision, and review and editing of the manuscript.

Funding

This study was funded by the Special Research Project of Traditional Chinese Medicine in Henan Province (2022ZY2031).

Conflict of Interest

The authors declare that there is no conflict of interest.

References

1 Global cancer burden growing, amidst mounting need for services. Saudi Med J 2024;45(03):326–327
2 Cancer Genome Atlas Research Network. Comprehensive molecular characterization of gastric adenocarcinoma. Nature 2014; 513(7517):202–209
3 Zhao AG, Cao W, Xu Y, et al. Survival benefit of an herbal formula for invigorating spleen for elderly patients with gastric cancer. J Chin Integr Med 2010;8(03):224–230
4 Zhu XH, Zhao AG, Li HW, et al. TCM Syndrome differentiation and treatment based on invigorating spleen for patients with stage IIIC gastric cancer after curative surgery. Chin Cancer 2016;25 (07):569–574
5 Xu Y, Zhao AG, Li ZY, et al. Survival benefit of traditional Chinese herbal medicine (a herbal formula for invigorating spleen) for patients with advanced gastric cancer. Integr Cancer Ther 2013; 12(05):414–422
6 Thompson A, Schäfer J, Kuhn K, et al. Tandem mass tags: a novel quantification strategy for comparative analysis of complex protein mixtures by MS/MS. Anal Chem 2003;75(08):1895–1904
7 Zhao AG, Yang JK, You SF, et al. Effects of Chinese herbal recipe Weichang'an in inducing apoptosis and related gene expression in human gastric cancer grafted onto nude mice. J Chin Integr Med 2007;5(03):287–297
8 Chiou SH, Lee KT. Proteomic analysis and translational perspective of hepatocellular carcinoma: Identification of diagnostic protein biomarkers by an onco-proteogenomics approach. Kaohsiung J Med Sci 2016;32(11):535–544
9 Burton LJ, Rivera M, Hawsawi O, et al. Muscadine grape skin extract induces an unfolded protein response-mediated autophagy in prostate cancer cells: a TMT-based quantitative proteomic analysis. PLoS One 2016;11(10):e0164115

10 Latosinska A, Vougas K, Makridakis M, et al. Comparative analysis of label-free and 8-plex iTRAQ approach for quantitative tissue proteomic analysis. PLoS One 2015;10(09):e0137048
11 te Velthuis AJW, Bagowski CP. PDZ and LIM domain-encoding genes: molecular interactions and their role in development. Sci World J 2007;7:1470–1492
12 Tamura N, Ohno K, Katayama T, et al. The PDZ-LIM protein CLP36 is required for actin stress fiber formation and focal adhesion assembly in BeWo cells. Biochem Biophys Res Commun 2007;364 (03):589–594
13 Chen HN, Yuan K, Xie N, et al. PDLIM1 stabilizes the E-cadherin/β-catenin complex to prevent epithelial-mesenchymal transition and metastatic potential of colorectal cancer cells. Cancer Res 2016;76(05):1122–1134
14 Li YM, Wei X, Li HZ, et al. Inhibition of the migration and invasion of glioblastoma multiforme U87 cells by RNAi silencing PDZ and LIM domain protein 1. Guangdong Yixue 2017;38(04):497–500
15 McNeely S, Beckmann R, Bence Lin AK. CHEK again: revisiting the development of CHK1 inhibitors for cancer therapy. Pharmacol Ther 2014;142(01):1–10
16 Cole KA, Huggins J, Laquaglia M, et al. RNAi screen of the protein kinome identifies checkpoint kinase 1 (CHK1) as a therapeutic target in neuroblastoma. P Natl Acad Sci USA 2011;108(08): 3336–3341
17 Liu B, Qu J, Xu F, et al. MiR-195 suppresses non-small cell lung cancer by targeting CHEK1. Oncotarget 2015;6(11):9445–9456
18 Kumar G, Breen EJ, Ranganathan S. Identification of ovarian cancer associated genes using an integrated approach in a Boolean framework. BMC Syst Biol 2013;7:12
19 Summers KM, Bokil NJ, Baisden JM, et al. Experimental and bioinformatic characterisation of the promoter region of the Marfan syndrome gene, FBN1. Genomics 2009;94(04):233–240
20 Sengle G, Tsutsui K, Keene DR, et al. Microenvironmental regulation by fibrillin-1. PLoS Genet 2012;8(01):e1002425
21 Yadin DA, Robertson IB, McNaught-Davis J, et al. Structure of the fibrillin-1 N-terminal domains suggests that heparan sulfate regulates the early stages of microfibril assembly. Structure 2013;21(10):1743–1756
22 Ma X, Wei J, Zhang L, et al. miR-486-5p inhibits cell growth of papillary thyroid carcinoma by targeting fibrillin-1. Biomed Pharmacother 2016;80:220–226
23 Zhang W, Ota T, Shridhar V, et al. Network-based survival analysis reveals subnetwork signatures for predicting outcomes of ovarian cancer treatment. PLOS Comput Biol 2013;9(03):e1002975
24 Cheng Q, Yuan F, Lu F, et al. CSIG promotes hepatocellular carcinoma proliferation by activating c-MYC expression. Oncotarget 2015;6(07):4733–4744
25 Li XP, Jiao JU, Lu LI, et al. Overexpression of ribosomal L1 domain containing 1 is associated with an aggressive phenotype and a poor prognosis in patients with prostate cancer. Oncol Lett 2016; 11(04):2839–2844
26 Ramaswamy S, Ross KN, Lander ES, Golub TR. A molecular signature of metastasis in primary solid tumors. Nat Genet 2003;33(01):49–54
27 Wolf K, Alexander S, Schacht V, et al. Collagen-based cell migration models in vitro and in vivo. Semin Cell Dev Biol 2009;20(08): 931–941
28 Yasui W, Oue N, Ito R, et al. Search for new biomarkers of gastric cancer through serial analysis of gene expression and its clinical implications. Cancer Sci 2004;95(05):385–392
29 Li AQ, Si JM, Shang Y, et al. Construction of COL1A1 short hairpin RNA vector and its effect on cell proliferation and migration of gastric cancer cells. Zhejiang Da Xue Bao Yi Xue Ban 2010;39(03): 257–263
30 Zhu B, Fukada K, Zhu H, et al. Prohibitin and cofilin are intracellular effectors of transforming growth factor beta signaling in human prostate cancer cells. Cancer Res 2006;66(17): 8640–8647
31 Atefi M, Avramis E, Lassen A, et al. Effects of MAPK and PI3K pathways on PD-L1 expression in melanoma. Clin Cancer Res 2014;20(13):3446–3457
32 Li M, Yin J, Mao N, et al. Upregulation of phosphorylated cofilin 1 correlates with taxol resistance in human ovarian cancer in vitro and in vivo. Oncol Rep 2013;29(01):58–66
33 Martoglio AM, Tom BD, Starkey M, et al. Changes in tumorigenesis- and angiogenesis-related gene transcript abundance profiles in ovarian cancer detected by tailored high density cDNA arrays. Mol Med 2000;6(09):750–765
34 Castro MA, Dal-Pizzol F, Zdanov S, et al. CFL1 expression levels as a prognostic and drug resistance marker in nonsmall cell lung cancer. Cancer 2010;116(15):3645–3655
35 Wang W, Mouneimne G, Sidani M, et al. The activity status of cofilin is directly related to invasion, intravasation, and metastasis of mammary tumors. J Cell Biol 2006;173(03):395–404
36 Pan J, Lin J, Izzo JG, et al. Genetic susceptibility to esophageal cancer: the role of the nucleotide excision repair pathway. Carcinogenesis 2009;30(05):785–792
37 García-Closas M, Malats N, Real FX, et al. Genetic variation in the nucleotide excision repair pathway and bladder cancer risk. Cancer Epidemiol Biomarkers Prev 2006;15(03):536–542
38 Sheng S. The urokinase-type plasminogen activator system in prostate cancer metastasis. Cancer Metastasis Rev 2001;20(3–4):287–296
39 Schmitt M, Harbeck N, Thomssen C, et al. Clinical impact of the plasminogen activation system in tumor invasion and metastasis: prognostic relevance and target for therapy. Thromb Haemost 1997;78(01):285–296
40 Koensgen D, Mustea A, Klaman I, et al. Expression analysis and RNA localization of PAI-RBP1 (SERBP1) in epithelial ovarian cancer: association with tumor progression. Gynecol Oncol 2007;107(02):266–273
41 Serce NB, Boesl A, Klaman I, et al. Overexpression of SERBP1 (Plasminogen activator inhibitor 1 RNA binding protein) in human breast cancer is correlated with favourable prognosis. BMC Cancer 2012;12:597
42 Baguley BC. Multiple drug resistance mechanisms in cancer. Mol Biotechnol 2010;46(03):308–316
43 Lin L, Yee SW, Kim RB, et al. SLC transporters as therapeutic targets: emerging opportunities. Nat Rev Drug Discov 2015;14 (08):543–560
44 Heise M, Lautem A, Knapstein J, et al. Downregulation of organic cation transporters OCT1 (SLC22A1) and OCT3 (SLC22A3) in human hepatocellular carcinoma and their prognostic significance. BMC Cancer 2012;12:109
45 Gotovdorj T, Lee E, Lim Y, et al. 2,3,7,8-tetrachlorodibenzo-p-dioxin induced cell-specific drug transporters with acquired cisplatin resistance in cisplatin sensitive cancer cells. J Korean Med Sci 2014;29(09):1188–1198
46 Huang Y, Anderle P, Bussey KJ, et al. Membrane transporters and channels: role of the transportome in cancer chemosensitivity and chemoresistance. Cancer Res 2004;64(12):4294–4301
47 Murrow L, Debnath J. ATG12-ATG3 connects basal autophagy and late endosome function. Autophagy 2015;11(06):961–962
48 Zhou XG, Han YH, Dang Q, et al. Effects of Atg3 and autophagy on cell migration in non-small cell lung cancer A549. Can Res Prev Treat 2017;44(08):525–529
49 Liu B, Wen X, Cheng Y. Survival or death: disequilibrating the oncogenic and tumor suppressive autophagy in cancer. Cell Death Dis 2013;4(10):e892
50 Galluzzi L, Pietrocola F, Bravo-San Pedro JM, et al. Autophagy in malignant transformation and cancer progression. EMBO J 2015; 34(07):856–880